PHYSICAL REVIEW C VOLUME 49, NUMBER 4 APRIL 1994

Global systematics of unique parity quasibands in odd-A collective nuclei

D. Bucurescu, G. Căta-Danil, M. Ivaşcu, L. Stroe, and C.A. Ur
Institute of Atomic Physics, P.O. Box MG-6, Bucharest, Romania
(Received 14 December 1993)

All known structures in the collective medium and heavy odd-A nuclei, based on the unique parity orbitals $g_{9/2}$, $h_{11/2}$, and $i_{13/2}$, are collected and correlations between the energies within both the favored and unfavored quasibands are analyzed. A first startling result is that irrespective of the nature of the odd particle and the shell model orbital, for most of the nondeformed nuclei the energies within these quasibands show a universal behavior of an anharmonic vibrator with a constant anharmonicity, identical with that found for the even-even nuclei. Second, the rapid transition between the anharmonic vibrator and the rotor regimes, which takes place in the even-even nuclei, is accompanied, in the adjacent odd-A nuclei, by an equally rapid transition from the anharmonic vibrator to the strong coupling regime.

PACS number(s): 21.10.Re, 21.10.Pc, 21.60.Ev

In contrast with the even-even nuclei, there are practically no attempts to approach the structure of the odd-A nuclei in a global way, by looking at the evolution of, or correlations between, certain observables which can be followed over practically all nuclei. This method has been applied quite succesfully to the even-even nuclei and led to a unified view of the evolution of the nuclear structure, from "pre-collective" nuclei to various transitional and collective behaviors [1,2]. However, while the even-even nuclei present a "standard" structure at low excitations [3] , in the odd-A nuclei, by varying the number of nucleons, one finds a diversity of level structures, as the odd nucleon spans different (deformed) shell model orbitals. For this reason, one usually compiles local systematics, in which a certain structure is followed over a restricted nuclear region, most often for a chain of isotopes or isotones.

The unique parity orbitals (UPO) offer, nevertheless, a special opportunity to make global investigations. In the odd-A nuclei, they give rise to structures which are readily recognized and assigned experimentally; also, at the lowest excitations (of the one-quasiparticle type) these levels have a pure structure, since the underlying UPO does not mix with other shell model orbitals. There are a few previous attempts to analyze the structural evolution of odd-A nuclei by using the UPO's as a probe, but these are restricted to a limited number of nuclei, in the mass region 80–100 and 130 [4–6].

The purpose of this Rapid Communication is to present global, phenomenological systematics of quasibands in odd-A nuclei based on three UPO's: $g_{9/2}$, $h_{11/2}$, and $i_{13/2}$.

With these three UPO's we span almost the entire nuclide chart, from medium to heavy nuclei. In the present analysis we leave aside the "shell model" nuclei, i.e. those which are close to at least one magic number. Besides this restriction, we analyze data from all known UPO structures. The $g_{9/2}$ structures that we consider are observed from $A\sim 60$ to $A\sim 100$; $\nu g_{9/2}$ from Ge to Mo, $\pi g_{9/2}$ from As to Ag. With $h_{11/2}$ one covers the mass regions from $A\sim 100$ to $A\sim 190$: $\nu h_{11/2}$ from Ru to Dy, $\pi h_{11/2}$ from Cs to Ir. The $i_{13/2}$ is observed in the neutron-odd nuclei from Nd to Pt. Some $\pi i_{13/2}$ structures are also observed in the actinides [7] but could not be included in the present analysis since they are usually low-K bands in which the observables that we follow up in all the other nuclei are usually not known. All the experimental data used in this phenomenological analysis were extracted from the Nuclear Data Sheets collection, from Ref. [8] and, in a few cases, from other published sources.

In all these nuclei we have followed two structures. The first is the so-called "favored" quasiband, which has the spin sequence $j, j+2, j+4, \ldots$, where j is the spin of the considered UPO. Most of the existing data concern this quasiband, which often constitutes the yrast sequence of "unique" parity and thus parallels the quasiground band (QGB) in the even-even nuclei. Second, we considered the sequence $j-1, j+1, j+3, \ldots$, which we denote, in the following, as the "unfavored" quasiband. We shall keep the terminology of "favored" and "unfavored" even in the case of the well deformed nuclei which realize the "strong coupling" situation [9] ,when actually both of them make part of a single band with rotational type energy spacings and spins $K, K+1, K+2, \ldots$, based on an intrinsic Nilsson state with angular momentum projection K on the symmetry axis.

It is of interest to remind briefly the characteristics of these quasibands in a few limiting situations [10]. In the "weak coupling" limit, the favored quasiband is practically identical with the QGB of the even-even core, and the unfavored states are almost degenerate with the favored ones. In the "decoupled" (or "rotation alignment") case, the favored quasiband is also identical with the QGB of the core, and the unfavored band is pushed upwards with respect to the favored one. In the "strong coupling" (or "deformation alignment") case, the two structures are interwoven into a $\Delta J=1$ rotational band; characteristic is that the energy differences within the two $\Delta J=2$ structures are rather large in comparison with those from the ground state band of the core. Thus, in the favored band, the energies of the states of spin

$j+2$, $j+4$, $j+6$ (relative to the state of spin j) are expressed (in units $\hbar^2/2\mathcal{J}$), as $(4j+6)$, $(8j+20)$, $(12j+42)$; compared to the energies of the states 2^+, 4^+, 6^+ in the ground state band of the core, which are 6, 20, 42 (in the same units), one has a considerable stretching of this band in the case of the UPO's with rather large j values considered here.

The experimental data show many cases when the considered quasibands show "transitional" characteristics, which differ from these well-known limiting situations, and there are many model approaches which explain the observed deviations by a multitude of factors. We do not attempt any model analysis, but inspect energy correlations within the experimental quasibands, from which global systematics emerge. Before showing the results, we make one last point: since in the odd-A nuclei there is no structural parameter which tells unambiguously when the deformation sets in, such as $R_{4/2} = E(4_1^+)/E(2_1^+)$ in the even-even nuclei, we classify the odd-A nuclei from this point of view according to the character of their even-even neighbors as follows. For each odd-mass nucleus we define its "core" as one of its neighbors, according to the particle—or hole—type of its odd nucleon and then use the $R_{4/2}$ values of the cores to classify. This definition of the "core" has nothing to do with any nuclear model—it is just a practical way to distinguish approximately the deformed nuclei from the ones which are not deformed.

Figure 1 shows plots of the energies of the states of spin $(j+4)$ and $(j+6)$ from the favored band against that of the state of spin $(j+2)$ (all energies relative to the state of spin j), for all the nuclei that have cores with $2.0 \leq R_{4/2} < 3.1$. These plots are the analogues of those recently considered in the even-even nuclei, $E(4_1^+)$ and $E(6_1^+)$ against $E(2_1^+)$ [1]. What is startling in Fig. 1 is that in both cases the global behavior observed is linear, although we mix together nuclei from many mass regions, and in addition, quasibands determined by two different UPO's : $1g_{9/2}$ and $1h_{11/2}$. Moreover, this linear behaviour coincides, within errors, with that of the anharmonic vibrator (AHV) with nearly constant anharmonicity which describes the corresponding core nuclei [1]. We thus find that the $(j+4)$ state behaves like a two-phonon state:

$$E(j+4) = \alpha E(j+2) + \epsilon_4 \quad (1)$$

with $\alpha = 1.99 \pm 0.03$ and $\epsilon_4 = 182 \pm 19$ keV (compared to the values of Ref. [1] of 2.02 ± 0.02 and 156 ± 10 keV, respectively). "Local" systematics are also compatible with the AHV behavior; thus, for the four cases we get, separately, $\nu g_{9/2}$: $\alpha = 1.83 \pm 0.11$, $\epsilon_4 = 328 \pm 95$; $\pi g_{9/2}$: $\alpha = 1.83 \pm 0.12$, $\epsilon_4 = 324 \pm 90$; $\nu h_{11/2}$: $\alpha = 1.95 \pm 0.09$, $\epsilon_4 = 194 \pm 44$; $\pi h_{11/2}$: $\alpha = 1.73 \pm 0.12$, $\epsilon_4 = 270 \pm 40$. For the global plot shown in Fig. 1, although there are several points with somewhat larger deviation, the overall scatter is statistical, consistent with a normal distribution with a 1σ deviation from the line of 6%. Similar conclusions are drawn for the higher states. Thus, for the state $(j+6)$ we find

$$E(j+6) = \beta E(j+2) + \epsilon_6 \quad (2)$$

with $\beta = 2.84 \pm 0.12$ and $\epsilon_6 = 564 \pm 52$, therefore compatible with the values $\beta = 3.0$ and $\epsilon_6 = 3\epsilon_4$ required by the AHV formula [11]. The scatter of the points here is larger, corresponding to a 1σ deviation of 9%. For the $(j+8)$ state we also get a global linear dependence, with slope 3.94 ± 0.23 (compatible with 4.0) and intercept 920 ± 114 keV (marginally compatible with $6\epsilon_4$), therefore, again, compatible with the AHV prediction.

The $\nu i_{13/2}$ structure is consistent with the above picture too. But the points representing this case are not included into Fig. 1 since most of the nuclei for which this structure is known are either "transitional" or deformed and are presented separately, in detail, later.

The number of known unfavored quasibands is smaller. One can see in Fig. 2 that this quasiband shows reasonably well the same AHV behavior.

The results of Figs. 1 and 2 are rather surprising. We expect these results in the weak coupling and decoupling cases. But, as shown in Fig. 3, there are many nuclei which deviate considerably from these limits, and even in a nonsystematic manner, such that one does not expect

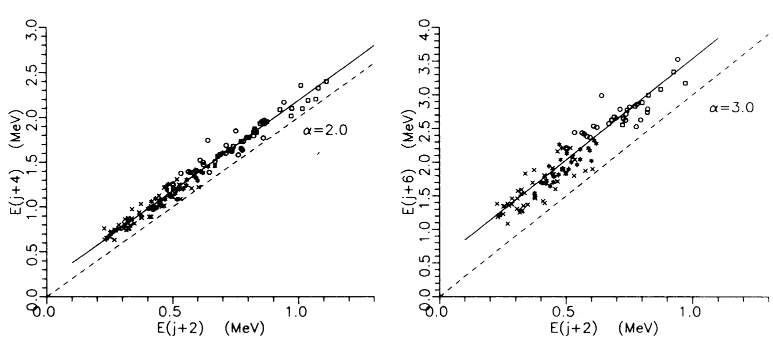

FIG. 1. Plots of the energy of the state of spin $j+4$ (left) and of the state of spin $j+6$ (right) against the energy of the state of spin $j+2$ (energies relative to the state of spin j; all states from the favored band). For the $j+4$ plot, the linear least-squares fit [Eq. (1)] with the parameters $\alpha = 1.99 \pm 0.03$ and $\epsilon_4 = 182 \pm 19$ keV is shown, while for the $j+6$ state the solid line is the calculated line $3.0E(j+2) + 3\epsilon_4$, as expected for the three-phonon state of an AHV. The dashed lines represent harmonic vibrator values. The meaning of the symbols is the following: squares: $\nu g_{9/2}$ band (Ge to Mo nuclei); circles: $\pi g_{9/2}$ (As to Ag); stars: $\nu h_{11/2}$ (Ru to Dy); crosses: $\pi h_{11/2}$ (Cs to Ir). In this figure only "collective" nondeformed nuclei have been selected (with cores having $2.0 \leq R_{4/2} < 3.1$, see also the text).

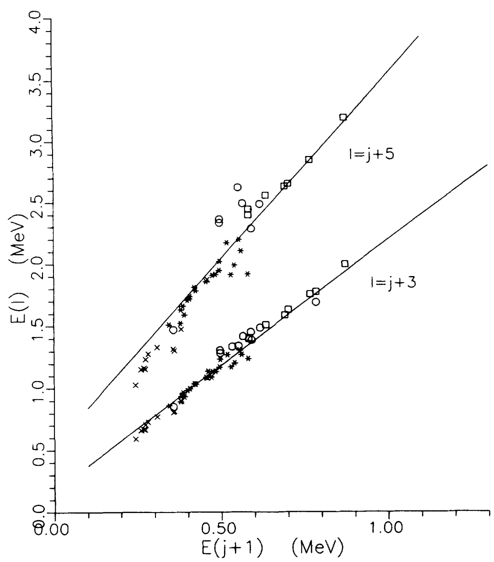

FIG. 2. The same as in Fig. 1, but for the energy of third and fourth states in the unfavored band $j-1, j+1, j+3, \ldots$ against the energy of the second state. The solid lines are the linear fits from the case of the favored band (the parameters given in the text).

the data in Figs. 1 and 2 to be so well correlated.

The results from Figs. 1 and 2 can be summed up as follows: by adding up one nucleon, in a UPO, to the even-even nuclei which have a universal AHV behavior [1] , one modifies, in certain cases, the phonon energy, but the unique AHV behavior is preserved for the energies of the favored band, and, as much as one can check on existing data, also for the unfavored band. As in the case of the even-even nuclei, although the internal structure of the implied phonon varies considerably [as shown by the $E(j+2)$ energy], the interaction energy between the phonons is always the same, being equal, within the errors, with that found for the even-even nuclei.

Next, we add into the picture the deformed nuclei and see how they connect to the data shown in Figs. 1 and 2. This is shown in Fig. 4 for the favored band. It is seen that by adding these deformed nuclei ($R_{4/2} \geq 3.1$) a second branch emerges besides the one represented by the AHV. Mainly the $\pi h_{11/2}$ structure defines this branch, since practically all known cases of deformed nuclei (among those represented in Fig. 4) belong to this case. The strong coupling (SC) limit describes quite well this second branch; for the $h_{11/2}$ orbital, the SC predictions shown in Fig. 4 are the straight lines with the slopes $(8j+20)/(4j+6) = 2.29$ [for the $(j+4)$ state] and $(12j+42)/(4j+6) = 3.86$ [for the $(j+6)$ state], respectively, and of intercept zero. Figure 4 may be misleading, however, concerning the way the transition between the AHV and SC regimes takes place, as it gives the impression that by decreasing $E(j+2)$ along the AHV line one meets a bifurcation point whereat some nuclei continue the AHV behavior and some others the SC one. In fact, this transition is more intricate, as one can see in Fig. 5. The details of this transition are especially clear in the case of the $\nu i_{13/2}$ structure, where it happens that most of the nuclei for which the favored band is known cover both sides: the AHV and the SC. One can observe that for all the six isotope chains presented one starts on the AHV line; then, with decreasing $E(j+2)$ the points depart gradually from this line and reach a "turning" point where the curve changes rapidly its direction by almost 180^o and then approaches the SC line by increasing $E(j+2)$ values. The corresponding $E(4_1^+)$ against $E(2_1^+)$ plot in the core nuclei is characterized by a continuous decrease in $E(4_1^+)$ as $E(2_1^+)$ decreases [1]. A plot of $E(j+2)$ versus $R_{4/2}$ of the core shows that the turn-

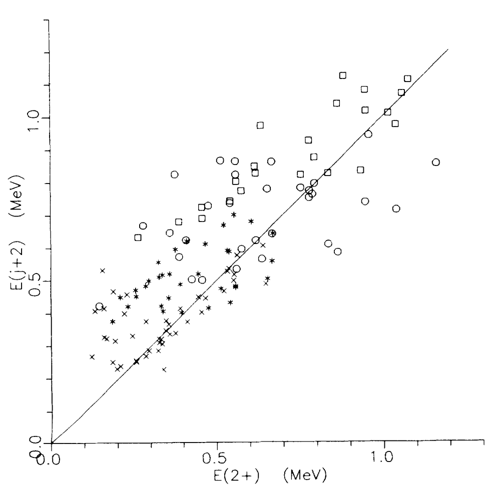

FIG. 3. Plot of the energy of the first excited state in the favored ban d as a function of that of the 2_1^+ state in the "core" nucleus (see text for definition of the core). The nuclei plotted here are the same with those from Fig. 1. The line is $E(j+2) = E(2_1^+)$.

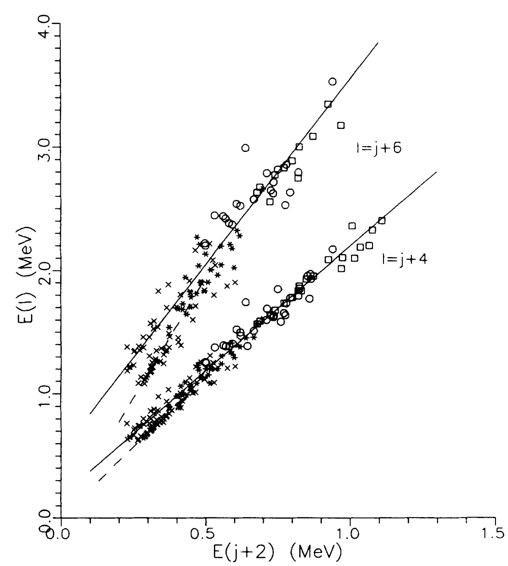

FIG. 4. Same as in Fig. 1 but with deformed nuclei [defined in the text a s those having $R_{4/2}$(core) ≥ 3.1] added. The solid lines are those from Fig. 1, while the dashed lines are calculated in the strong coupling limit, for the $h_{11/2}$ case: $E(j+4) = 2.29E(j+2)$ and $E(j+6) = 3.86E(j+2)$, respectively.

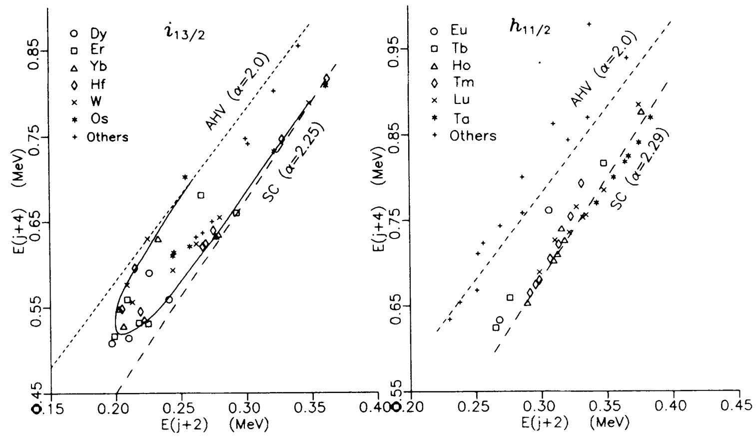

FIG. 5. Details of the transition from the AHV to the SC regime, for the $\nu i_{13/2}$ case (left) and $\pi h_{11/2}$ (right). The AHV behavior is calculated with $\alpha = 2.00$ and $\epsilon_4 = 182$ keV [Eq. (1)]. The solid line in the $i_{13/2}$ plot is drawn by hand through the points to illustrate the typical way the AHV $\rightarrow$ SC transition takes place. For the $i_{13/2}$ case, the only known additional points concern four $N = 87$ isotones (Sm, Gd, Dy, Er) which deviate from the general pattern (being below both the AHV and SC lines).

ing point region (which, for $i_{13/2}$, is at about 200 keV) is defined by those nuclei whose cores pass through values $R_{4/2}$ of $\sim 3.0 - 3.15$, therefore to the narrow region where the derivative $dE(4_1^+)/dE(2_1^+)$ undergoes a very rapid change from 2.0 to 3.33, which has the characteristics of a critical phase transition [1]. The AHV $\rightarrow$ SC transition in the odd-A nuclei is also characterized by a rapid variation of the derivative $dE(j+4)/dE(j+2)$, which is even discontinuous at the turning point. In Fig. 5 one can see that the AHV $\rightarrow$ SC transition for the $h_{11/2}$ structure also takes place through a turning point (around 300 keV), although here most of the known nuclei lie already on the SC line.

The origin of the turning point is the following. In the AHV regime, generally, by decreasing $E(2_1^+)$, $E(j+2)$ decreases at first. Decreasing $E(2_1^+)$ further, one finally reaches the rotor regime which forces the SC regime to set up in the adjacent odd nuclei. Approaching the SC limit, however, means a strong increase of $E(j+2)$ [since one tends towards the SC limit, $E(j+2) = \frac{4j+6}{6}E(2_1^+)$, which is $5.33E(2_1^+)$ for the $i_{13/2}$ case], which actually turns the slow decrease of $E(2_1^+)$ into an increase of $E(j+2)$ (although very few nuclei actually reach the SC limit).

To summarize, we have been able to show that for all the odd-A collective nuclei, with $Z = 32$ to $Z = 78$, the evolution of the favored and unfavored quasibands determined by unique parity orbitals ($g_{9/2}$, $h_{11/2}$, $i_{13/2}$) follows a remarkable parallelism with that of the quasiground band in the even-even nuclei. First, in the nondeformed nuclei, the energies within these quasibands show universal correlations which are described by an anharmonic vibrator with nearly constant anharmonicity, which is identical with that found for the even-even nuclei, and this is independent of the mass region and the orbital involved.

Second, the rapid (critical phase) transition between the anharmonic vibrator and rotor regimes in the even-even nuclei is reflected in the odd-A nuclei into a rapid transition from the anharmonic vibrator to the strong coupling regime, which takes place around a turning point in the plot of the energy of the state of spin $j+4$ against the energy of the state of spin $j+2$.

The present results show that, according to the structures based on the unique parity orbitals, all the collective odd-A nuclei fall into two classes, the anharmonic vibrator and the strong coupling regimes, which pass one into the other within a narrow zone of rapid transition.

The present global systematics are of much interest for predictions in the new nuclear regions. It would be equally interesting to check whether this classification applies as well to the one-quasiparticle level structures based on other shell model orbitals.

[1] R. F. Casten, N. V. Zamfir, and D. S. Brenner, Phys. Rev. Lett. **71**, 227 (1993).
[2] R. F. Casten, N. V. Zamfir, and D. S. Brenner, presented at the Symposium "Capture Gamma-Ray Spectroscopy", Fribourg, 1993 (unpublished).
[3] M. Sakai, At. Data Nucl. Data Tables **31**, 399 (1986).
[4] H. Dejbakhsh, Phys. Lett. B **210**, 50 (1988).
[5] S. L. Tabor, Phys. Rev. C **34**, 311 (1986)
[6] D. Bucurescu, G. Cata, E. Dragulescu, M. Ivascu, N. V. Zamfir, A. Gizon, and J. Gizon, Phys. Lett. B **229**, 321 (1989).
[7] K. Jain and A. K. Jain, At. Data Nucl. Data Tables **50**, 269(1992).
[8] *Table of Isotopes,* edited by C. M. Lederer and V. S. Shirley 7th ed. (Wiley, New York, 1978).
[9] F. S. Stephens, Rev. Mod. Phys. **47**, 43 (1975).
[10] P. Ring and P. Schuck, *The Nuclear Many-Body Problem* (Springer, New York, 1980).
[11] D. M. Brink, A. F. R. de Toledo Piza, and A. K. Kerman, Phys. Lett. **19**, 413 (1965).